Materials Physics and Mechanics 24 (2015) 278-283 Received: November 5, 2015

CRITICAL THICKNESS AND BOW OF PSEUDOMORPHIC $In_xGa_{1-x}As$-BASED LASER HETEROSTRUCTURES GROWN ON (001)GaAs AND (001)InP SUBSTRATES

M.E. Rudinsky[1], S.Yu. Karpov[1,2*], H. Lipsanen[2,3], A.E. Romanov[2,4]

[1]STR Group – Soft-Impact, Ltd., P.O. Box 83, 27 Engels ave., St. Petersburg, 194156, Russia

[2]ITMO University, 49 Kronverkskiy ave., Saint Petersburg, 197101, Russia

[3]Aalto University, FI–00076 Aalto, Finland

[4]Ioffe Physical-Technical Institute, 26 Polytechnicheskaya str., Saint Petersburg, 194021, Russia

*e-mail: sergey.karpov@str-soft.com

Abstract. Using the energy-balance approach, we have estimated critical thickness for misfit dislocation (MD) formation and wafer bow for single- and multi-layer InGaAs-based pseudomorphic heterostructures used in light-emitting devices. Indicating the onset of stress relaxation via MD formation, the analysis of critical thicknesses serves as a guideline for device structure design avoiding extensive defect generation usually accompanying the relaxation. Estimates of structure bow are helpful for meeting requirements of the wafer post-growth processing technology. Suggested methodology may be applied to optimization of strain-compensated semiconductor laser heterostructures.

1. Introduction

Bandgap engineering, including strain management, has become a powerful approach to development of state-of-the-art optoelectronic and electronic devices. It was successfully applied to reducing threshold current density of III-V semiconductor laser diodes [1], improving characteristics of pseudomorphic high electron mobility transistors [2], developing optoelectronic devices based on intra-band optical transitions, like intersubband infrared photo-detectors [3] and quantum-cascade lasers [4], expanding spectral range of tandem solar cells [5], etc. In optoelectronic devices, light-emitting diodes and laser diodes, the use of strained quantum well (QW) active regions enables smart choice of the most suitable semiconductor materials [6] and proper adjusting of the emission wavelength to practically important spectral ranges [7].

On the other hand, the use of strained layers creates additional problems. The first one is the well-known problem of misfit and threading dislocation (MD and TD) formation during the growth of strained epitaxial layers. In light-emitting diodes and laser diodes, MDs (and TDs) generated near (and in) the active region reduce substantially the internal quantum efficiency of the devices and lead to their accelerated degradation. In electronic devices, like high-electron mobility transistors, the dislocations enhance scattering of two-dimensional electrons, thus lowering their mobility and drift velocity. Therefore, avoiding dislocation formation in the strained device heterostructures is a key point of their design. The second problem is bowing of the grown wafers induced by built-in elastic strains. The bowing is undesirable for post-growth device processing, as well as for the life-time of the devices in course of their operation.

In order to prevent the dislocation generation and diminish bow of strained

heterostructures, the so-called strain-compensated structures have been suggested, see, for instance, [8-11]. It has been demonstrated that such structures possess improved surface morphology, much lower defect density, and better optical properties, as compared to conventional strained structures. Being introduced empirically, the strain-compensated structures proved to be quite promising for practical applications. However, no comprehensive theoretical analysis of general principles of such structures design has been, to our knowledge, reported in literature to date.

In the present study, we suggest a methodology for estimating critical thickness of MD formation in an arbitrary multi-layer strained epitaxial structure and to apply it to analysis of phosphorus-free pseudomorphic InGaAs-based laser heterostructures on (001)GaAs and (001)InP substrates intended for light emission in various spectral ranges. Bowing of the structures induced by the elastic strain is also discussed in the paper, as an important technological factor.

2. Modeling methods

In order to estimate the critical thickness h_c of MD formation, we used the energy-balance approach similar to that suggested in Refs. [12-14]. Gliding of 60°-dislocations with the Burgers vector $\boldsymbol{b} = (a/2)\langle 011\rangle$ in the easy-slip {111} planes was considered as the basic mechanism of MD generation. According to the energy-balance approach, the MDs started to form, if the work of the biaxial mismatch stress W_{str} exceeded the self-energy of the dislocation W_{dis}. Procedure of W_{str} and W_{dis} calculation had been discussed in detail in [13]. The results of h_c calculation depended generally on the biaxial elastic moduli M and Poisson's ratio ν of all the layers, which were derived from the elastic constants C_{ij} of cubic semiconductors as follows:

$$M = C_{11} + C_{12} - 2C_{12}^2 / C_{11} \ , \quad \nu = C_{12} / (C_{11} + C_{12}) \tag{1}$$

The stiffness constants of binary III-V compounds were known from experiments [15], whereas those of ternary and quaternary compounds, e.g. $In_xGa_{1-x}As$ were interpolated between the binary ones using the Vegard's rule. The mismatch stress in every epitaxial layer was estimated, assuming pseudomorphic growth of the layer on a chosen substrate and accounting for its particular lattice constant mismatch with the substrate.

Important point in calculation of W_{dis} is the choice of the dislocation core radius R_c which cannot be estimated on the basis of elasticity theory only. Earlier studies carried out for ionic crystals showed that R_c variation between $b/2$ and $2b$ fitted well the available observations [16]. On the other hand, $R_c = b/4$ was recommended in [17] for covalent semiconductors, providing, in particular, excellent quantitative agreement between the theoretical predictions and measured critical thicknesses of pseudomorphic SiGe alloys grown on silicon substrates. We had also chosen the latter value of the dislocation core radius, since it predicted the critical thickness of ~0.9 nm for InAs grown on (001)GaAs, being in good agreement with experimental findings, 0.7-1.0 nm obtained by precise measurements enabled in molecular beam epitaxy [18, 19].

Curvature of the whole wafer including the substrate and all the epitaxial layers was estimated by general approach suggested in [20]. In the case of a single layer on a substrate, this approach reduced to a well-known Stoney's formula [21].

3. Critical thickness of InGaAs quantum wells and wafer bow

Figure 1 compares predicted h_c values for MD formation for single $In_xGa_{1-x}As$ layers with various compositions coherently grown on either (001)InP or (001)GaAs substrates. In the case of the $In_xGa_{1-x}As$/GaAs structures, h_c decreases dramatically with the InAs molar fraction x and becomes as small, as $h_c \approx 7$ nm near the practically important value $x = 0.22$ (see Fig. 1a) corresponding to active regions of semiconductor lasers emitting at the wavelength of 980 nm.

This implies the active regions of such lasers to include a single QW with the width less than the above found h_c. At higher x, the critical thickness diminishes to $h_c \approx 0.9$ nm in the case of pure InAs/GaAs.

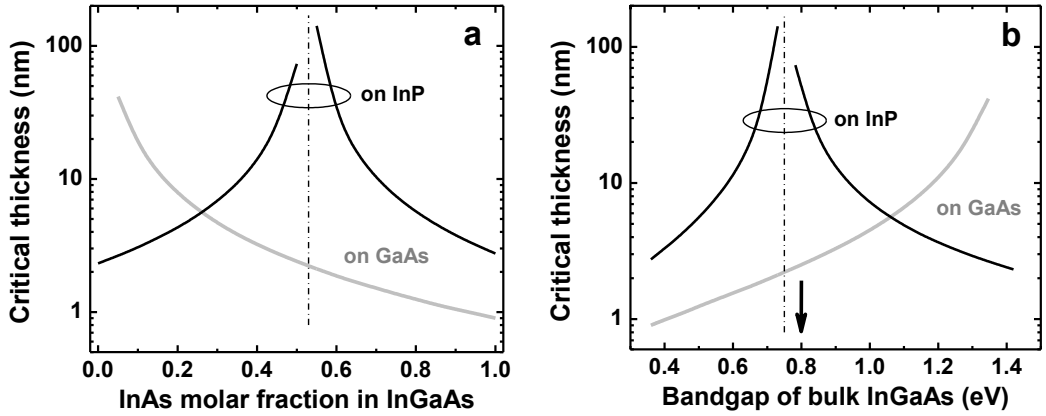

Fig. 1. Critical thickness h_c of a single pseudomorphic $In_xGa_{1-x}As$ layer grown on either (001)InP or (001)GaAs substrate as a function of (a) alloy composition and (b) bandgap of bulk unstrained semiconductor. Dash-dotted line marks the composition of the alloy lattice-matched to InP. Vertical arrow indicates the bandgap corresponding to the emission wavelength of 1.55 μm.

The critical thicknesses of $In_xGa_{1-x}As$ grown on InP and GaAs becomes $h_c \approx 5.5$ nm at the InAs molar fraction $x = 0.26$. For layers with $x > 0.26$ grown on InP substrates, the critical thickness rises up and goes to infinity at $x = 0.53$ corresponding to InGaAs lattice-matched with InP and then decreases monotonically to the value $h_c \approx 2.8$ nm for InAs/InP.

Figure 1b shows h_c plotted as a function of bandgap of unstrained $In_xGa_{1-x}As$. The vertical arrow in the figure indicates the bandgap corresponding to the emission wavelength of 1.55 μm. At this bandgap, $h_c \approx 50$ nm, i.e. a quasi-bulk single layer may be chosen as the active region of light-emitting device with such wavelength. The latter estimate is based, however, on the spectral properties of the bulk unstrained $In_xGa_{1-x}As$ alloys. In practice, thin single and multiple QWs (SQWs and MQWs) are employed in the laser diodes. Here, the lattice constant mismatch and the electron/hole quantum confinement result in the optical transition energies remarkably higher than the bandgap of the bulk materials. To compensate the joint effect of strain and quantum confinement, the QWs with increased Indium content are exploited. Estimates show that the bandgap of the bulk $In_xGa_{1-x}As$ should be shifted to ~0.6-0.7 eV (x = 0.57-0.67), depending on QW width. This corresponds to h_c=10-60 nm that limit the allowable widths of the QWs used in the device structures.

To analyze wafer bow, we have considered a representative heterostructure containing five strained 4 nm InGaAs QWs sandwiched between other lattice-matched layers, which were grown on a 350 μm (001) substrate made of either GaAs or InP. As the substrate thickness is much larger than the total thickness of the whole heterostructure, only the total thickness of the strained QWs but not the individual thicknesses of other layers is expected to determine the bow value. Figure 2 shows the wafer curvatures K as a function of the $In_xGa_{1-x}As$ composition estimated by the approach mentioned in Sec. 2. The structure lattice-matched with InP provides zero curvature, whereas positive and negative curvatures correspond to the concave and convex wafer bending, respectively. The curvature of the structure with $x = 0.22$ grown on GaAs substrates is: $K = -15$ km^{-1}. That of the structures with x = 0.57-0.67 grown on InP, suitable for QW-based optoelectronic devices operating in the 1.55 μm spectral range, is varied between -2 and -10 km^{-1}.

A typical stage of the post-growth processing of semiconductor laser diodes is thinning of the substrate to ~100-120 μm prior separation of the wafer into individual laser bars. In this

case, the curvature increases approximately by an order of magnitude, in accordance to the Stoney's formula [20]. Such a curvature results in the wafer bow up to 60-70 μm for the wafer diameter of 2 inches and initial curvature $|K|$ ~10 km^{-1} of the 350 μm substrate.

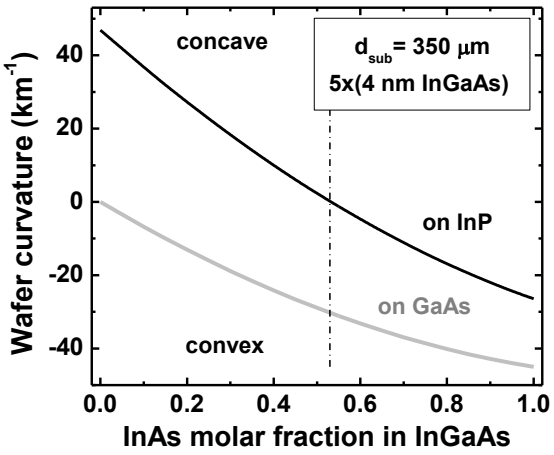

Fig. 2. Wafer curvature of the structures containing five strained 4 nm $In_xGa_{1-x}As$ QWs grown on either (001)GaAs or (001)InP substrates as a function of composition. Dash-dotted line marks the composition of the alloy lattice-matched to InP.

4. Strain compensation in multi-layer structures

The results discussed in the previous section serve as a guideline for the choice of suitable SQW composition and width preventing the well from stress relaxation. In practice, however, MQWs are frequently employed as the active regions of laser diodes. The MQW structures have critical thicknesses different from those of SQW structures due to a lower effective stress σ_{eff}, which is the driving force for dislocation gliding:

$$\sigma_{eff} = h_{tot}^{-1} \sum_s \sigma_s h_s \quad , \quad h_{tot} = \sum_s h_s \quad , \tag{2}$$

where σ_s is the biaxial stress in the s-th epitaxial layer, h_s is the thickness of the layer, and summation in Eq.(2) is performed over all the layers in the MQW structure. One can see from Eq. (2), in particular, that the effective stress in an MQW structure with the barriers lattice-matched to the underlying substrate (zero stress in the barrier layers) is always less than in the SQW structure with the thickness equal to the total width of all the strained QWs.

Of practical interest is estimation of the maximum number of QWs that can be grown without stress relaxation. For this purpose, we find a critical QW amount as the sequent number of the QW in the MQW structure, counted from bottom to top, in which the relaxation starts to occur. The number of QWs that is possible to grow without stress relaxation is less than that critical QW number by unity.

Figure 3 shows by dotted line the critical QW number estimated for the MQW structure with the 3.7 nm InGaAs QWs and 3.9 nm $In_{0.53}Ga_{0.47}As$ barriers lattice-matched with the InP substrate. As expected, the critical QW number grows dramatically near the $In_xGa_{1-x}As$ QW composition corresponding to lattice matching with InP. In the range of the alloy composition x = 0.57-0.67 discussed above, the critical QW number varies between 4 and 10. This means that the number of QWs in the structure free of plastic relaxation should be limited by the value of 3-9, depending on the choice of the specific $In_xGa_{1-x}As$ composition.

For comparison, we have examined a strain-compensated MQW structure differing from the above one only by the barrier material, $In_{0.40}Ga_{0.45}Al_{0.15}As$ instead of $In_{0.53}Ga_{0.47}As$. The effective stress in this structure becomes equal to zero at x = 0.67. The dependence of the critical QW number on the InGaAs QW composition computed for the strain-compensated structure

becomes shifted to higher x compared to that of the structure with the lattice-matched $In_{0.53}Ga_{0.47}As$ barriers. In particular, the critical QW number in the practically interesting range x = 0.57-0.67 is predicted to vary from 6 to infinity. So, the use of the strain-compensated MQW structure enables substantial increase in the allowable number of QWs to be grown without stress relaxation.

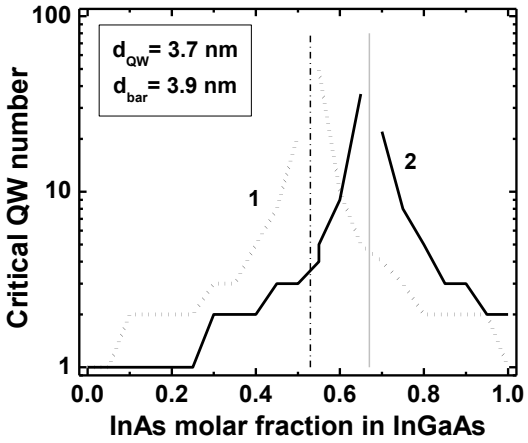

Fig. 3. Critical QW number in a pseudomorphic MQW structure on (001)InP substrate as a function of InGaAs composition: 1 – structure with the QW barriers lattice-matched with InP, 2 – structure with strain-compensating $In_{0.40}Ga_{0.45}Al_{0.15}As$ barriers. Dash-dotted line marks the material lattice-matched with InP. Grey solid line indicates the quasi-matching conditions corresponding to zero effective stress (see text for details).

The advantages of strain-compensated structures resulting from possibility of controlling the quasi-matching of lattice constants (σ_{eff} = 0) are evident, if the mismatch stresses in both QWs and barriers are not so high. At high stresses, alternative relaxation mechanisms come into the play, like those studied in [22], leading eventually to extended defect formation. Determination of the workability range of strain-compensated structures is a task for future studies.

5. Conclusions

Using the energy-balance approach extended to the case of multi-layer heterostructures, we have estimated critical thickness and wafer bow for a set of pseudomorphic InGaAs-based structures on (001)GaAs and (001)InP substrates, close to those used for fabrication of light-emitting devices. For this purpose one of the model parameters, namely the dislocation core radius, has been adjusted to fit the critical thickness of the InAs layers on (001)GaAs substrate measured precisely during molecular beam epitaxy growth.

The estimates of the critical thicknesses provided for single $In_xGa_{1-x}As$ layers may serve as guideline for the choice of the width and composition of strained InGaAs QWs suitable for light emission in a practically important spectral ranges, on the one hand, and free from stress relaxation, on the other hand. The wafer bending predicted for a typical MQW structure is found to be rather substantial, which should be taken into account in post-growth processing of optoelectronic devices, such as light-emitting diodes and laser diodes.

Critical QW numbers corresponding to the onset of stress relaxation have been estimated for typical InGaAs MQW active regions of the laser diodes with the lattice-matched and strain-compensated barriers. The $In_xGa_{1-x}As$ composition "window" suitable for growth of relaxation-free MQW structures with a large number of QWs has been identified. The shift of the "window" predicted for the strain-compensated structure is controlled by quasi-matching conditions corresponding to zero effective stress.

In view of the demonstrated practical advantages of using strain-compensated heterostructures, analysis of alternative mechanisms of stress relaxation that limit their workability seems to be of primary importance for future studies. Morphological undulation of the growth surface accompanied by the local generation of extended defects is expected to be one of such mechanisms.

Acknowledgment

This work is supported by the Ministry of Education and Science of Russian Federation within the federal program "Research and development in priority directions of elaboration of science and technology in Russia for 2014-2020 years"; code 2015-14-582-0038, grant No 14.581.21.0013 from 4 August, 2005; unique identificator RFMEFI58115X0013.

References

[1] E. Yablonovitch, E.O. Kane // *Journal of Lightwave Technology* **6** (1988) 1292.
[2] J.J. Rosenberg, M. Benlamri, P.D. Kirchner, J.M. Woodall, J.D. Pettit // *IEEE Electron Device Letters* **6** (1985) 491.
[3] A.G.U. Perera, S.G. Matsik, In: *Intersubband Infrared Photodetectors*, ed. by V. Ryzhii (World Scientific Publishing Co. Pte. Ltd, Singapore, 2003), p. 229.
[4] M.A. Belkin, F. Capasso // *Physica Scripta* **90** (2015) 118002.
[5] J.G.J. Adams, B.C. Browne, I.M. Ballard, J.P. Connolly, N.L.A. Chan, A. Ioannidis, W. Elder, P.N. Stavrinou, K.W.J. Barnham, N.J. Ekins-Daukes // *Progress in Photovoltaics: Research and Applications* **19** (2011) 865.
[6] A. Klehr, F. Bugge, G. Erbert, J. Fricke, A. Knauer, P. Ressel, H. Wenzel, G. Tränkle // *Proceedings of SPIE* **6133** (2006) 96.
[7] R. Liang, J. Chen, G. Kipshidze, D. Westerfeld, L. Shterengas, G. Belenky // *IEEE Photonics Technology Letters* **23** (2011) 603.
[8] C. Ellmers, M.R. Hofmann, D. Karaiskaj, S. Leu, W. Stolz, W.W. Rühle, M. Hilpert // *Applied Physics Letters* **74** (1999) 1367.
[9] N. Georgiev, T. Dekorsy, F. Eichhorn, M. Helm, M.P. Semtsiv, W.T. Masselink // *Applied Physics Letters* **83** (2003) 210.
[10] C.A. Wang, A. Goyal, R. Huang, J. Donnely, D. Galawa, G. Turner, A. Sanchez-Rubio, A. Hsu, Q. Hu, B. Williams // *Journal of Crystal Growth* **312** (2010) 1157.
[11] W.Y. Jiang, B. Chen, J. Yuan, A.L. Holmes, Jr. // *Proceedings of SPIE* **7660** (2010) 76603O.
[12] J.W. Matthews, A.E. Blackeslee // *Journal Crystal Growth* **27** (1974) 118.
[13] L.B. Freund // *Journal of Applied Mechanics* **54** (1987) 553.
[14] M.Yu. Gutkin, A.L. Kolesnikova, A.E. Romanov // *Materials Science and Engineering* **A164** (1993) 433.
[15] J.Y. Tsao, *Materials Fundamentals of Molecular Beam Epitaxy* (Academic Press, Inc., San Diego, 1993).
[16] I. Vurgaftman, J.R. Meyer, L.R. Ram-Mohan // *Journal of Applied Physics* **89** (2001) 5815.
[17] J. Friedel, *Dislocations* (Pergamon Press, Oxford, 1964).
[18] A. Mazuelas, L. Gonzalez, L. Tapfer, F. Briones // *MRS Proceedings* **263** (1992) 473.
[19] A. Sasaki // *Thin Solid Films* **267** (1995) 24.
[20] L.B. Freund // *Journal of Crystal Growth* **132** (1993) 341.
[21] G.G. Stoney // *Proceedings of the Royal Society of London A* **82** (1909) 172.
[22] N.N. Ledentsov, V.A. Shchukin, S. Rouvimov // *Applied Physics Letters* **104** (2014) 033106.